International Psychogeriatrics (2016), 28:9, 1503–1511 © International Psychogeriatric Association 2016
doi:10.1017/S1041610216000624

The effects of apolipoprotein ε 4 on aging brain in cognitively normal Chinese elderly: a surface-based morphometry study

Hanna Lu, Suk Ling Ma, Sandra Sau Man Chan and Linda Chiu Wa Lam

Department of Psychiatry, The Chinese University of Hong Kong, G/F Multicenter, Tai Po Hospital, Hong Kong, SAR China

ABSTRACT

Background: Default mode network (DMN) has been reported to be susceptible to APOE ε 4 genotype. However, the APOE ε 4-related brain changes in young carriers are different from the ones in elderly carriers. The current study aimed to evaluate the cortical morphometry of DMN subregions in cognitively normal elderly with APOE ε 4.

Method: 11 cognitively normal senior APOE ε 4 carriers and 27 matched healthy controls (HC) participated the neuropsychological tests, genotyping, and magnetic resonance imaging (MRI) scanning. Voxel-based morphometry (VBM) analysis was used to assess the global volumetric changes. Surface-based morphometry (SBM) analysis was performed to measure regional gray matter volume (GMV) and gray matter thickness (GMT).

Results: Advancing age was associated with decreased GMV of DMN subregions. Compared to HC, APOE ε 4 carriers presented cortical atrophy in right cingulate gyrus (R_CG) (GMV: APOE carriers: 8475.23 ± 1940.73 mm^3, HC: 9727.34 ± 1311.57 mm^3, $t = 2.314$, $p = 0.026$, corrected) and left insular (GMT: APOE ε 4 carriers: 3.83 ± 0.37 mm, HC: 4.05 ± 0.25 mm, $t = 2.197$, $p = 0.033$, corrected).

Conclusions: Our results highlight the difference between different cortical measures and suggest that the cortical reduction of CG and insular maybe a potential neuroimaging marker for APOE 4 ε senior carriers, even in the context of relatively intact cognition.

Key words: Apolipoprotein E, default mode network, surface-based morphometry, voxel-based morphometry, cingulate gyrus, insula

Introduction

Prevalence of dementia is expected to rise tremendously in an aging population over the coming decades (Alzheimer's Association, 2015). Since the interventions and treatments for dementia are unfavorable when the disease progresses to a later stage, it is crucial to identify the specific marker to differentiate healthy aging from the conditions associated with high risks of progressive neurodegeneration. Apolipoprotein E (APOE) ε 4 allele, one of the well-replicated genetic risk factor for sporadic AD (Corder, *et al.*, 1993; Saunders *et al.*, 1993; Liu *et al.*, 2013), has been reported to participate the formulation of β-amyloid (Aβ) (Mahley *et al.*, 2006). Given the evidence of positron emission tomography (PET) studies, the Aβ deposition in specific brain regions is a pathological hallmark of Alzheimer's disease (AD) (Buckner *et al.*, 2005; Bero *et al.*, 2011).

Notably, the organizations under these specific anatomical regions are referring to a crucial modularity, that is the default mode network (DMN) (Fox *et al.*, 2005; Sperling *et al.*, 2009). DMN refers to a set of brain regions that demonstrates reduced activity during attention-demanding tasks and increased activity during resting state (Buckner and Vincent, 2007). Beyond the network level, the DMN subregions present two classes of features: (1) the first class is that the default network regions, coordinating as a system, engage in various cognitive processes (Beckmann *et al.*, 2005; Smith *et al.*, 2009) and interact with other brain network (i.e. salience network) (Uddin *et al.*, 2015); (2) the second class is that each DMN subregions plays critical roles in specific cognitive functions. For instance, dorsolateral prefrontal cortex (DLPFC) involved in decision making (Szczepanski and Knight, 2014), hippocampus formation (HF) involved in memory (Wikenheiser

Correspondence should be addressed to: Dr. Hanna Lu Address, Department of Psychiatry, The Chinese University of Hong Kong, G/F Multicenter, Tai Po Hospital, Tai Po, Hong Kong. Phone: +(852) 6464-1397; Fax: +(852) 2667-5464. Email: hannalu@cuhk.edu.hk. Received 5 Nov 2015; revision requested 7 Dec 2015; revised version received 14 Mar 2016; accepted 17 Mar 2016. First published online 21 April 2016.

https://doi.org/10.1017/S1041610216000624 Published online by Cambridge University Press

and Redish, 2012), CG involved in cognitive control and attention (Leech and Sharp, 2014). This "two-level" feature of DMN raises the question of whether APOE ε 4 allele affects the cortical morphometry of default network regions generally or regionally? A number of VBM studies has shown that hippocampus (Lemaître *et al.*, 2005), medial temporal cortex (Honea *et al.*, 2009; Taylor *et al.*, 2014), and frontotemperal region (Wishart *et al.*, 2006) are vulnerable to APOE ε 4 – related pathology. Further, enhanced investigation of cortical morphology has benefited from the advances of SBM analysis. Similar to VBM findings, cortical reduction has been found in entorhinal cortex (Shaw *et al.*, 2007), anterior cingulate, and lateral temporal cortices (Alexander *et al.*, 2012) in young APOE ε 4 carriers (i.e. age range 25–45). However, some studies focusing on the middle-aged APOE ε 4 carriers (i.e. age range 44–48) have reported no APOE ε 4 effects on cortical thickness of DMN subregions (Bunce *et al.*, 2012), reduced cortical thickness in frontal regions (Fennema-Notestine *et al.*, 2011), or even a thicker cortical thickness in temporal regions (Espeseth *et al.*, 2008). It seems that the interactive dynamics between APOE ε 4 and brain morphometry present an age-specific property. Indeed, some studies have reported that APOE ε 4 has an impact on accelerating the cortical reduction in healthy aging elderly (Chen *et al.*, 2007; Espeseth *et al.*, 2008; Shi *et al.*, 2014).

Considering the inevitable brain changes in aging (Walhove *et al.*, 2011), it is not easy to answer whether APOE has a specific effect on DMN subregions in elderly carriers. Besides of age, the poor-matched baseline in terms of gender and education could strongly influence the brain morphometry and lead to the mixed results as well. Hence, the present study has two aims: (1) To assess the global volumetric difference between APOE ε 4 carriers and matched HC. (2) To quantitatively evaluate and compare the GMV and GMT of DMN subregions. To achieve the objectives, VBM would be used to detect the global brain volume, and SBM would be conducted to evaluate the regional GMV and GMT. Based on previous findings, we would hypothesize that APOE ε 4 carriers would present cortical reduction of DMN subregions. Moreover, we also expected that the defaults network regions with morphometric changes in APOE ε 4 carriers would be associated with clinical features.

Materials and methods

Participants

Thirty-eight community-dwelling Chinese older adults aged from 65–80 years were recruited from another cohort study that aims to establish a detailed characterization of cognitive and healthy profiles of Chinese older adults and to determine the diagnostic markers for preclinical dementia (Lam *et al.*, 2015). Potential participants 65 and older were firstly scheduled for a 1.5-hour in-person interview and APOE genotyping at the research center. Further, the eligible participants were invited to participate the MRI scanning. During the on-site interview, the participants received a structured questionnaire of medical history and a neuropsychological battery. Ethics approval was obtained from the Joint Chinese University of Hong Kong-New territories East Cluster Clinical Research Ethics Committee. Written informed consent from all participants was obtained before the cognitive assessments and APOE genotyping.

Apolipoprotein E genotyping

All participants provided a sample of DNA for APOE genotyping. Genomic DNA was extracted from peripheral blood samples using DNA extraction kit according to the instruction (Qiagen, US). The presence of APOE ε 2, APOE ε 3, and APOE ε 4 alleles were analyzed and performed using PCR-RFLP, which was well validated and described in our previous work (Ma *et al.*, 2005).

Cognitive assessments and clinical evaluation

A standardized neuropsychological battery was used to evaluate the global cognition and major domains of cognition (Lu *et al.*, 2015). The battery was administered by trained research assistants and the scores were calculated by two independent raters. Cantonese Mini-Mental State Examination (CMMSE) and Alzheimer's Disease Assessment Scale (ADAS) (Chu *et al.*, 2000) were used as a global measure of cognitive function. Delayed recall of words: the number of recalled words was used as the performance of episodic memory. Chinese verbal fluency test (CVFT): the average number of the unique words within a semantic category in 1 minute was used as a measure of executive function. Trail making tests (TMT): the participants had to connect either numbers (A), or numbers and letters in an alternate fashion (B) as fast as possible; the time of completing in seconds was used as a measure of attention (TMT-A) and executive function (TMT-B). Digit span tests: the participants had to repeat the numbers they heard, either forward or backward; the number of correct repeated numbers was used as a measure of attention (DSF) and a measure of working memory

https://doi.org/10.1017/S1041610216000624 Published online by Cambridge University Press

(DSB) (Lam *et al.*, 2005). All the measures were conducted with Chinese instructions.

Magnetic resonance imaging acquisition

3D high-resolution MR images were acquired in Prince of Wales Hospital (Hong Kong) with a 3.0 Tesla Philips scanner (Philips Medical System, Best, the Netherlands). The scanning time for each participant was 8.5 minute. T1-weighted MRI data set was configured with the following acquisition parameters: axial acquisition with a 256 × 256 × 192 matrix, thickness = 1 mm, no gap, field of view (FOV) = 230 mm, TR = 2070 ms, TE = 3.93 ms, flip angle = 15°. The sequence yielded high quality isotropic images with the voxel size of 1 mm × 1 mm × 1 mm.

Voxel-based morphometry (VBM) analysis

Quality check of T1 images, pre-processing, and optimal VBM analysis were performed by VBM8 toolbox (http://dbm.neuro.uni-jena.de/vbm/) running on MATLAB (MATLAB R2012b, The Math Works Inc. Natick, MA) with default parameters (Good *et al.*, 2001). The processing included the following steps: (1) All anatomical images were reoriented by anterior and posterior (AC-PC) line manually; (2) Images were bias-corrected, tissue classified, and registered using linear (12-parameter affine) and non-linear transformations (warping), within a unified model (Ashburner and Friston, 2005); (3) The segmentation procedure from the VBM8 toolbox produced gray matter (GM), white matter (WM) and registered rigid-body aligned tissue segments for each image in the Montreal Neurological Institute (MNI) space; (4) Modulation of different tissue segments by nonlinear normalization parameters to account for the differences of individual brain size globally; (5) The normalized and modulated GMV were smoothed with a Gaussian kernel of 8 mm full width at half maximum (FWHM).

Surface-based morphometry (SBM) analysis

Cortical morphometry, including GMV and GMT, were calculated by BrainSuite 14.0 (http://brainsuite.org/). BrainSuite is an automatic cortical surface identification integrated package with the updated version of Brain Surface Extraction (BSE) and friendly interface (Shattuck and Leahy, 2002; Pantazis *et al.*, 2010), which are widely used in dementia and aging studies (Frisoni *et al.*, 2009; Apostolova *et al.*, 2010; Hwang *et al.*, 2013).

To calculate regional GMV and GMT individually, we followed the standard pipeline and default parameters (Shattuck *et al.*, 2008). The SBM analysis was obtained by submitting each participant's MRI to a series of steps, including: (1) motion correction; (2) intensity normalization; (3) removal of non-brain voxels; (4) segmentation of GM, WM, and cerebrospinal fluid (CSF); (5) tessellation of the GM/WM boundary, and automated topology correction. At each step, the results were visually inspected and manual interventions were performed when required to correct topological defects. Cortical image processing was conducted by the investigators blinded to subjects' demographics, APOE ε 4 statuses, and cognitive performance.

Statistical analysis

First, group differences of demographics, cognitive performance, voxel-wise GM differences were tested either with χ^2 for categorical variables or with independent two samples *t*-test for continuous variables. Second, regional GMV and GMT were calculated individually. We followed the Cendes methods (Cendes *et al.*, 1993) to adjust the heterogeneity of head size and conducted a correction of individual variance of total intracranial volume (TIV) through the following formula: Corrected SV = (MBV × SV)/IBV. MBV is the mean brain volume in the group (which is a constant), SV is the regional volume of GM, and IBV is the individual brain volume. Third, the group-wise comparisons of GMV and GMT were conducted using the code embedded in MATLAB (http://neuroimage.usc.edu/neuro/Resources/BST_SVReg_Utilities). Multiple comparison correction was performed by the above code using false discovery rate (FDR) estimation (Reiter *et al.*, 2012). Person's correlation was used to detect the relationship between age, cognitive functions, and regional morphometry of DMN subregions. Bonferroni correction was used to reduce chances of obtaining false-positive results of correlation analysis (Jiang *et al.*, 2004; Watanabe *et al.*, 2013). Given the six pairs of ROI, the statistical significant level would be 0.05/12 = 0.0042. The χ^2 test, two sample *t*-test, and Person's correlation were performed by IBM SPSS Statistics (Version 20).

Results

Demographics and Cognitive performance

As shown in Table 1, the demographics in term of age, gender, years of education were similar between APOE ε 4 carriers and healthy group. The global cognition and cognitive functions cross the main domains between two groups were also comparable. While, there was a trend that APOE ε 4 carriers presented worse cognitive performance than HC.

https://doi.org/10.1017/S1041610216000624 Published online by Cambridge University Press

Table 1. Demographics and cognitive performance of APOE ε 4 carriers and healthy controls

	APOE ε 4 CARRIERS ($N = 11$)	HEALTHY CONTROLS ($N = 27$)	t VALUE	p VALUE
Age	69.48 ± 4.41	70.40 ± 4.35	0.584	0.913
Gender (F/M)	7/4	17/10	−0.038	0.970
Education in years	7.00 ± 4.27	8.48 ± 3.88	1.038	0.306
CMMSE	27.36 ± 3.00	27.81 ± 2.39	0.490	0.627
ADAS	7.36 ± 2.25	6.19 ± 2.86	−1.220	0.230
Delayed recall	6.09 ± 1.30	6.67 ± 1.52	1.101	0.278
DSB	3.63 ± 1.29	4.07 ± 1.84	0.719	0.477
DSF	7.09 ± 1.64	7.70 ± 1.23	1.260	0.216
CVFT	28.18 ± 7.92	28.85 ± 5.05	0.313	0.756
Trail making test A	13.27 ± 7.88	15.70 ± 10.45	0.381	0.706
Trail making test B	17.27 ± 10.64	20.56 ± 14.00	0.698	0.490

Note: Data are raw scores and presented as mean ± SD. Abbreviations: CMMSE = Cantonese Mini-Mental State Examination; ADAS = Alzheimer's Disease Assessment Scale; DSB = Digit span backward; DSF = Digit span forward; CVFT = Chinese verbal fluency test.

Table 2. Comparisons of GMV of default network regions in APOE carriers and healthy controls

DEFAULT NETWORK REGIONS	HEMISPHERE	APOE ε 4 CARRIERS ($N = 11$)	HEALTHY CONTROLS ($N = 27$)	t VALUE	p VALUE
Medial prefrontal cortex (mPFC)	Left	11286.92 ± 2249.06	11415.55 ± 1740.93	0.190	0.851
	Right	10962.33 ± 2262.75	11661.29 ± 3316.94	0.638	0.527
Cingulate gyrus (CG)	Left	8345.18 ± 1652.19	9188.06 ± 1405.14	1.594	0.120
	Right	8475.23 ± 1940.73	9727.34 ± 1311.57	2.314	0.026
Precuneus gyrus (Pcu)	Left	8546.56 ± 1195.24	8655.09 ± 1239.77	0.247	0.806
	Right	8079.29 ± 1457.85	8001.46 ± 1176.91	−0.173	0.864
Inferior parietal lobule (IPL)	Left	10120.72 ± 1793.94	9537.49 ± 1478.07	−1.037	0.307
	Right	9692.23 ± 1769.00	9263.97 ± 1459.35	−0.772	0.445
Hippocampal formation (HF)	Left	1135.09 ± 584.96	1314.67 ± 383.08	1.120	0.364
	Right	1510.89 ± 557.45	1517.29 ± 315.44	0.045	0.972
Lateral temporal cortex (LTC)	Left	13657.67 ± 2118.29	14166.88 ± 1977.81	0.251	0.803
	Right	13657.67 ± 2118.29	14166.88 ± 1977.81	0.706	0.485

Note: Data are raw scores and presented as mean ± SD.

VBM results

With a threshold of uncorrected $p < 0.001$, there was no voxel left. Although the APOE ε 4 carriers demonstrated less GMV (APOE ε 4 carriers: 544.99 ± 38.06; HC: 557.90 ± 65.08, $t = 0.613$, $p = 0.543$) and WMV (APOE ε 4 carriers: 445.21 ± 52.27; HC: 459.50 ± 51.66, $t = 0.771$, $p = 0.446$), no significant difference was found between two groups.

SBM results

Based on the well-established neural underpinnings of DMN (Fox *et al.*, 2005; Buckner *et al.*, 2008), six pairs (left/right) of brain regions are selected as regions of interest (ROIs), including medial prefrontal gyrus (mPFC), CG, precuneus gyrus (Pcu), inferior parietal lobe (IPL), hippocampal formation (HF), and lateral temporal cortex (LTC). As Table 2 shown, APOE ε 4 carriers demonstrates a global cortical atrophy, but significant decreased GMV was found in right CG (Figure 1a) (APOE ε 4 carriers: 8475.23 ± 1940.73 mm^3, HC: 9727.34 ± 1311.57 mm^3, $t = 2.314$, $p = 0.026$, 95% CI [154.65, 2349.57], and reduced GMT was found in left insular (Figure 1b) (APOE ε 4 carriers: 3.83 ± 0.37 mm, HC: 4.05 ± 0.25 mm, $t = 2.197$, $p = 0.033$, 95% CI [0.007, 0.427]).

Associations between age, cognitive functions, and DMN subregions

Using gender, education and TIV as covariates, significant negative correlations (Figure 2) were found between age and subregions of DMN, including GMV of right IPL (2a. $r = -0.516$, $p = 0.001$) and left Pcu (2b. $r = -0.41$, $p = 0.013$). The results suggest that the cortical atrophy of DMN subregions is coupled with advancing age. With age, gender, and education as covariates, extensive associations were found between scores of cognitive functions and cortical morphometry of

https://doi.org/10.1017/S1041610216000624 Published online by Cambridge University Press

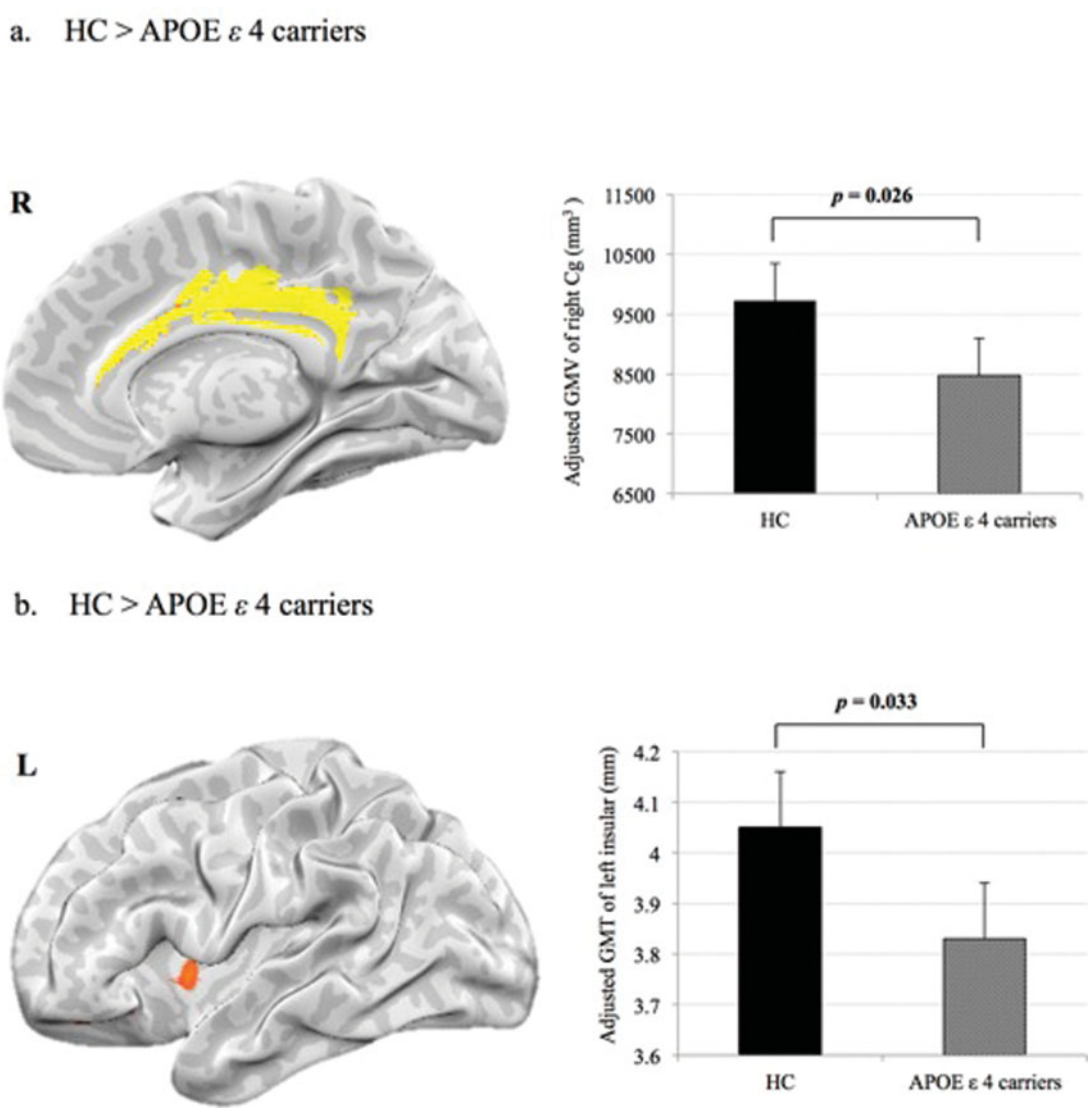


Figure 1. (Colour online) Inflated surface maps of the morphometric difference between APOE ε 4 and healthy groups. (a) depicts the medial view of right cingulate gyrus (Cg) and (b) depicts the lateral view of left insular.

DMN subregions (Figure 3). Short-term memory measured by DSB was positively correlated with right LTC (GMV: $r = 0.497$, $p = 0.002$; GMT: $r = 0.5$, $p = 0.002$) and right IPL (GMT: $r = 0.565$, $p < 0.001$). Executive function measure by CVFT was positively associated with right hippocampus (GMV: $r = 0.486$, $p = 0.003$).

Discussion

The current study was the first attempt to combine both VBM and SBM analysis to identify the morphometric changes of default network regions in Chinese senior adults with genetic risk for AD. Generally, the present study highlights the reduced cortical volume and thickness of DMN subregions in cognitively normal senior APOE ε 4 carriers.

Does APOE ε 4 have a preferential influence on DMN in old age?

It is a challenge to postulate the characteristic changes of brain morphometry in APOE ε 4 carriers with normal cognition. With regard to the accelerating effect of APOE ε 4, cortical changes were more pronounced in senior APOE ε 4 carriers than the younger ones (Papenberg, Lindenberger, and Bäckman, 2015). Evidence from functional MRI (fMRI) studies also confirmed the stronger APOE ε 4 effects on multiple DMN subregions in senior adults (Filippini *et al.*, 2011). It seems that APOE ε 4 has the differential effects on brain in young and old adults.

Even though it is very difficult to identify the pure APOE ε 4 effects, the well-matched baseline is necessary in the comparison and explanation of morphometric properties accounting for APOE

https://doi.org/10.1017/S1041610216000624 Published online by Cambridge University Press

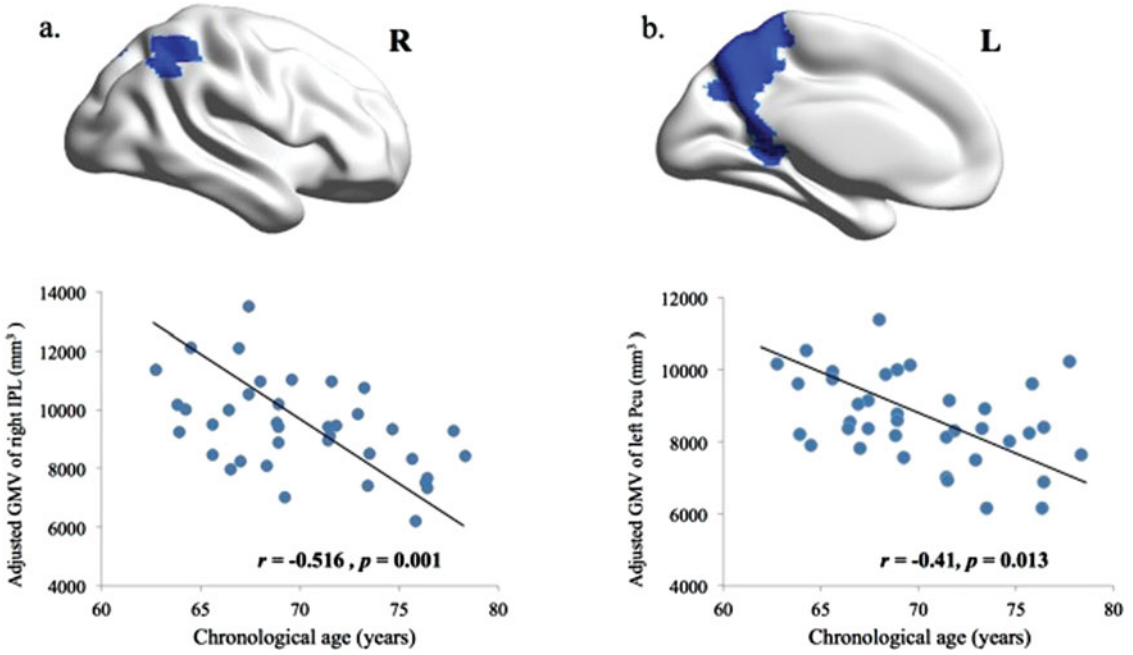


Figure 2. (Colour online) Scatterplot of the correlation between age and cortical morphometry.

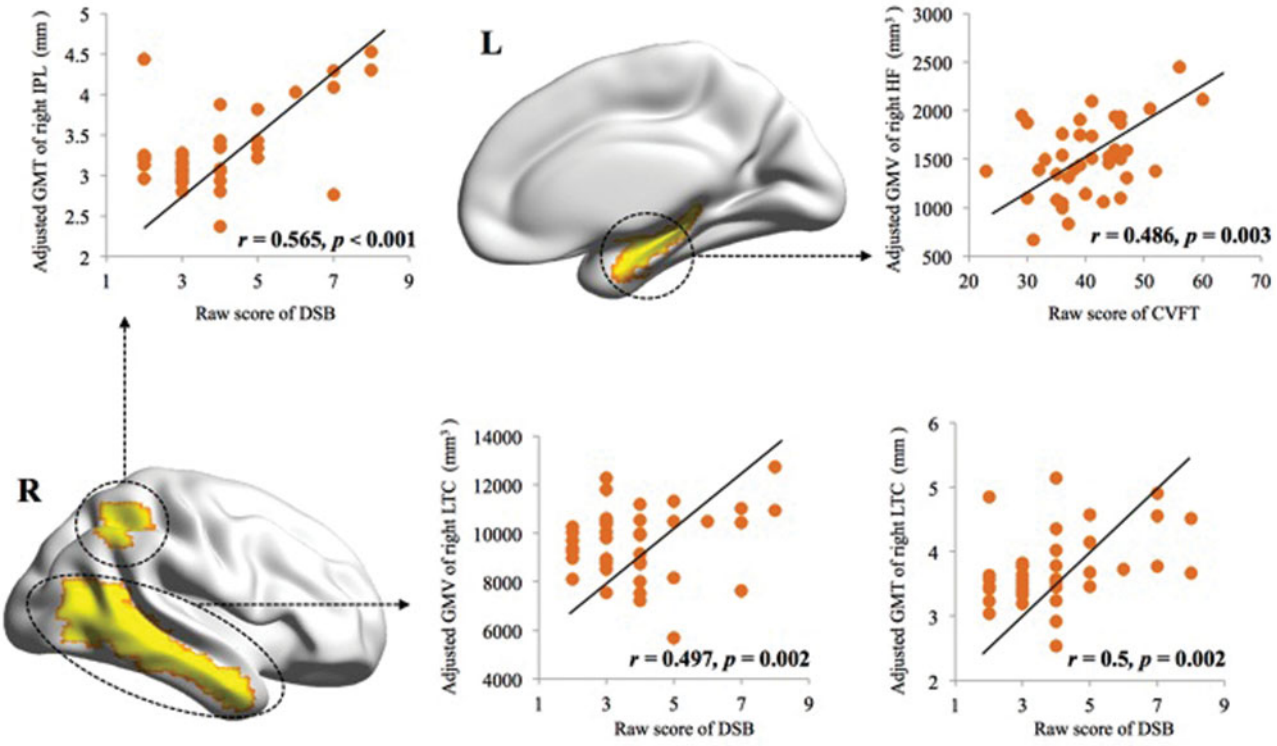


Figure 3. (Colour online) Scatterplot of the correlation between scores of cognitive functions and cortical morphometry.

ε 4. Thus, the question we addressed as whether APOE ε 4 has a differential effect on cortical properties of DMN subregions maybe revised as does APOE ε 4 have a preferential effect on DMN subregions in elderly carriers. In the continuum from cognitively normal APOE ε 4 carriers to preclinical stage of AD, DMN is vulnerable to be affected by healthy and pathological aging. Aligned with previous studies (Shiino *et al.*, 2006; Filippini *et al.*, 2009; Alexander *et al.*, 2012), it is not surprising that the prominent age-related atrophy was found in DMN subregions (Figure 2). In the comparison between APOE ε 4 carriers and HC, the significant morphometric difference was detected

https://doi.org/10.1017/S1041610216000624 Published online by Cambridge University Press

by SBM instead of VBM analysis. With particular interest, pronounced decreased GMV of right CG and reduced GMT of left insular have been found in APOE ε 4 carriers. The results indicate at least two things: (1) Morphometric property in terms of volumetric and cortical thickness may change in a nonlinear fashion in late adulthood (Westlye *et al.*, 2011). (2) APOE ε 4 may influence the cortical morphometric specifically rather than globally in the non-symptom stage.

APOE ε 4-related effects on cortical morphometry

Indeed, the mechanism that contributes to the regional changes within default mode regions in APOE ε 4 carriers has not been fully understood. The possible explanations could be postulated from two perspectives. Firstly, from the perspective of pathological vulnerability, the APOE ε 4 related brain regions with Aβ deposition are coordinated with the pathological process proposed by Braak's (Braak and Braak, 1991; De Leon *et al.*, 2001). Two hallmarks of AD-related pathology, neurofibrillary tangles (NFTs) and Aβ, are largely distributed in anterior insular context (Bonthius *et al.*, 2005) and CG (Sperling *et al.*, 2009) and at the early stage of AD. Besides the volumetric changes, reduced cortical thickness (Gutiérrez-Galve *et al.*, 2009) and WM lesions (Zhuang *et al.*, 2012) of CG have also been found in APOE 4 ε carriers. Furthermore, evidence from PET and magnetic resonance spectroscopy (MRS) studies also confirmed the decreased metabolism of CG (Reiman *et al.*, 2012; Gomar *et al.*, 2014) and insular (Yao *et al.*, 2015) in APOE 4 ε carriers, even several years before the onset of cognitive impairment. Second, from the perspective of functional anatomy, the multifaceted roles of CG and insular have been reported to engage across cognitive, affective, and behavioural contexts. CG, as a member of cortical midline structures (CMS), acts as a "hub" connecting multiple brain regions (Buckner and Krienen, 2013). Insular is one of the most frequently identified regions with degenerative change in AD. However, the heterogeneity within insular makes it very difficult to discuss the results across studies. Recent studies employing various methods appear to converge on the functional anatomy of insula into at least three distinct subregions (Chang *et al.*, 2013). One of them is the dorsoanterior region of insular, associating with higher cognitive processing and coordinating the interplay between DMN and salience network (Uddin *et al.*, 2015), which is compatible with the region presented reduced GMT in our results (Figure 1b).

As to the brain-behavior correlations, although the cortical morphometry were positively correlated with cognitive functions (Figure 3), we have not detected the relationship between CG, insular, and cognitive functions. The potential explanation might be due to the comparable scores of cognitive and clinical evaluation between APOE 4 ε and HC. Besides, the non-linear fashion of morphometric properties in late adulthood may affect the correlation results as well (Westlye *et al.*, 2011). In summary, our results highlight the difference between different cortical measures and suggest that the cortical reduction of CG and insular maybe a potential neuroimaging marker for APOE 4 ε senior carriers.

Limitations and future works

The findings of this study should be circumspectly interpreted with its limitations. First, the cortical properties of cingulate cortex subregions have not been launched due to the brain template embedded in BrainSuite. Second, cross-sectional design with a small sample size may limit the generalizability of the findings. Third, some cerebrovascular risk factors, such as blood pressure and cholesterol level, are not included in this study, which may affect the cortical morphometry as well. Fourth, only APOE genotype was tested as the genetic risk factor. Fifth, all participants were from Chinese community, which may not give an accurate reflection of the features of senior adults with various cultural backgrounds.

Given the lateralized feature of APOE ε 4-related change, it would be intriguing to investigate the potential APOE-related effects on cortical lateralization in two completely independent cohorts with healthy and pathological aging. Besides, it is crucial to validate our findings in a longitudinal cohort. Finally, the APOE ε 4-related regions in our finding could be used as the seeds to test the functional connectivity within DMN in the future studies by using resting state fMRI.

Conflict of interest

None.

Description of authors' roles

Hanna Lu, Sandra S.M. Chan, and Linda C.W. Lam conceived and designed this study. Hanna Lu performed the VBM and SBM analysis. Suk Ling Ma conducted the Apolipoprotein E genotyping of this study. Regarding to this paper, Hanna Lu drafted, Suk Ling Ma, Sandra S.M. Chan, and

https://doi.org/10.1017/S1041610216000624 Published online by Cambridge University Press

Linda C.W. Lam discussed and agreed the final version.

Acknowledgments

This research was supported by the Direct Grant from the Chinese University of Hong Kong. The authors would like to thank all the participants and their relatives that kindly agreed to participate in the study.

References

Alexander, G. E. *et al.* (2012). Gray matter network associated with risk for Alzheimer's disease in young to middle-aged adults. *Neurobiology of Aging*, 33, 2723–2732.

Apostolova, L. G. *et al.* (2010). Surface feature-guided mapping of cerebral metabolic changes in cognitively normal and mildly impaired elderly. *Molecular Imaging and Biology: MIB: The Official Publication of the Academy of Molecular Imaging*, 12, 218–224.

Ashburner, J. and Friston, K. J. (2005). Unified segmentation. *NeuroImage*, 26, 839–851.

Association, A. (2015). 2015 Alzheimer's disease facts and figures. *Alzheimer's & Dementia*, 11, 332–384.

Beckmann, C. F., DeLuca, M., Devlin, J. T. and Smith, S. M. (2005). Investigations into resting-state connectivity using independent component analysis. *Philosophical Transactions of the Royal Society B*, 360, 1001–1013.

Bero, A. W. *et al.* (2011). Neuronal activity regulates the regional vulnerability to amyloid-[beta] deposition. *Nature Neuroscience*, 14, 750–756.

Bonthius, D. J., Solodkin, A. and Van Hoesen, G. W. (2005). Pathology of the insular cortex in Alzheimer disease depends on cortical architecture. *Journal of Neuropathology & Experimental Neurology*, 64, 910–922.

Braak, H. and Braak, E. (1991). Neuropathological stageing of Alzheimer-related changes. *Acta Neuropathologica*, 82, 239–259.

Buckner, R. L. *et al.* (2005). Molecular, structural, and functional characterization of Alzheimer's disease: evidence for a relationship between default activity, amyloid, and memory. *The Journal of Neuroscience*, 25, 7709–7717.

Buckner, R. L., Andrews-Hanna, J. R. and Schacter, D. L. (2008). The brain's default network: anatomy, function, and relevance to disease. *Annals of the New York Academy of Sciences*, 1124, 1–38.

Buckner, R. L. and Krienen, F. M. (2013). The evolution of distributed association networks in the human brain. *Trends in Cognitive Sciences*, 17, 648–665.

Buckner, R. L. and Vincent, J. L. (2007). Unrest at rest: default activity and spontaneous network correlations. *Neuroimage*, 37, 1091–1096.

Bunce, D. *et al.* (2012). APOE genotype and entorhinal cortex volume in non-demented community-dwelling adults in midlife and early old age. *Journal of Alzheimer's Disease*, 30, 935–942.

Cendes, F., Andermann, F., Frcp, C., Gloor, P. and Evans, A. (1993). MRI volumetric measurement of amygdala and hippocampus in temporal lobe epilepsy. *Neurology*, 43(4), 719–725.

Chang, L. J., Yarkoni, T., Khaw, M. W. and Sanfey, A. G. (2013). Decoding the role of the insula in human cognition: functional parcellation and large-scale reverse inference. *Cerebral Cortex*, 23, 739–749.

Chen, K. *et al.* (2007). Correlations between apolipoprotein E ε4 gene dose and whole brain atrophy rates. *American Journal of Psychiatry*, 164, 916–921.

Chu, L. W. *et al.* (2000). The reliability and validity of the Alzheimer's disease assessment scale cognitive subscale (ADAS-Cog) among the elderly Chinese in Hong Kong. *Annals of the Academy of Medicine*, Singapore, 29, 474–485.

De Leon, M. J. *et al.* (2001). Prediction of cognitive decline in normal elderly subjects with 2-[18F] fluoro-2-deoxy-D-glucose/positron-emission tomography (FDG/PET). *Proceedings of the National Academy of Sciences of the United States of America*, 98, 10966–10971.

Espeseth, T. *et al.* (2008). Accelerated age-related cortical thinning in healthy carriers of apolipoprotein E ε4. *Neurobiology of Aging*, 29, 329–340.

Fennema-Notestine, C. *et al.* (2011). Presence of ApoE ε4 allele associated with thinner frontal cortex in middle age. *Journal of Alzheimer's Disease*, 26, 49–60.

Filippini, N. *et al.* (2009). Anatomically-distinct genetic associations of APOE epsilon4 allele load with regional cortical atrophy in Alzheimer's disease. *NeuroImage*, 44, 724–728.

Filippini, N. *et al.* (2011). Differential effects of the APOE genotype on brain function across the lifespan. *NeuroImage*, 54, 602–610.

Fox, M. D. *et al.* (2005). The human brain is intrinsically organized into dynamic, anticorrelated functional networks. *Proceedings of the National Academy of Sciences of the United States of America*, 102, 9673–9678.

Frisoni, G. B., Prestia, A., Rasser, P. E., Bonetti, M. and Thompson, P. M. (2009). In vivo mapping of incremental cortical atrophy from incipient to overt Alzheimer's disease. *Journal of Neurology*, 256, 916–924.

Gomar, J. J. *et al.* (2014). APOE genotype modulates proton magnetic resonance spectroscopy metabolites in the aging brain. *Biological Psychiatry*, 75, 686–692.

Good, C. D. *et al.* (2001). A voxel-based morphometric study of ageing in 465 normal adult human brains. *NeuroImage*, 14, 21–36.

Gutiérrez-Galve, L. *et al.* (2009). Patterns of cortical thickness according to APOE genotype in Alzheimer's disease. *Dementia and Geriatric Cognitive Disorders*, 28, 476–485.

Honea, R. A., Vidoni, E., Harsha, A. and Burns, J. M. (2009). Impact of APOE on the healthy aging brain: a voxel-based MRI and DTI study. *Journal of Alzheimer's Disease*, 18, 553–564.

Hwang, K. S. *et al.* (2013). Mapping cortical atrophy in Parkinson's disease patients with dementia. *Journal of Parkinson's Disease*, 3, 69–76.

Jiang, T., He, Y., Zang, Y. and Weng, X. (2004). Modulation of functional connectivity during the resting state and the motor task. *Hum Brain Mapp*, 22, 63–71.

Lam, L. C. *et al.* (2015). Intellectual and physical activities, but not social activities, are associated with better global cognition: a multi-site evaluation of the cognition and

https://doi.org/10.1017/S1041610216000624 Published online by Cambridge University Press

lifestyle activity study for seniors in Asia (CLASSA). *Age and Ageing*, 44, 835–840.

Leech, R. and Sharp, D. J. (2014). The role of the posterior cingulate cortex in cognition and disease. *Brain*, 137, 12–32.

Lemaître, H. *et al.* (2005). No epsilon4 gene dose effect on hippocampal atrophy in a large MRI database of healthy elderly subjects. *NeuroImage*, 24, 1205–1213.

Liu, C. C., Kanekiyo, T., Xu, H. and Bu, G. (2013). Apolipoprotein E and Alzheimer disease: risk, mechanisms and therapy. *Nature Reviews Neurology*, 9, 106–118.

Lu, H., Fung, A. W. T., Chan, S. S. M. and Lam, L. C. W. (2015). Disturbance of attention network functions in Chinese healthy older adults: an intra-individual perspective. *International Psychogeriatrics*, 9, 1–11.

Ma, S. L., Tang, N. L. S., Lam, L. C. W. and Chiu, H. F. K. (2005). The association between promoter polymorphism of the interleukin-10 gene and Alzheimer's disease. *Neurobiology of Aging*, 26, 1005–1010.

Mahley, R. W., Weisgraber, K. H. and Huang, Y. (2006). Apolipoprotein E4: a causative factor and therapeutic target in neuropathology, including Alzheimer's disease. *Proceedings of the National Academy of Sciences of the United States of America*, 103, 5644–5651.

Pantazis, D. *et al.* (2010). Comparison of landmark-based and automatic methods for cortical surface registration. *NeuroImage*, 49, 2479–2493.

Papenberg, G., Lindenberger, U. and Bäckman, L. (2015). Aging-related magnification of genetic effects on cognitive and brain integrity. *Trends in Cognitive Sciences*, 19, 506–514.

Reiman, E. M. *et al.* (2012). Brain imaging and fluid biomarker analysis in young adults at genetic risk for autosomal dominant Alzheimer's disease in the presenilin 1 E280A kindred: a case-control study. *Lancet Neurology*, 11, 1048–1056.

Reiter, K. *et al.* (2012). Cognitively normal individuals with AD parents may be at risk for developing aging-related cortical thinning patterns characteristic of AD. *NeuroImage*, 61, 525–532.

Saunders, A. M. *et al.* (1993). Association of apolipoprotein E allele 4 with late-onset familial and sporadic Alzheimer's disease. *Neurology*, 43, 1467–1472.

Shattuck, D. W. *et al.* (2008). Construction of a 3D probabilistic atlas of human cortical structures. *NeuroImage*, 39, 1064–1080.

Shattuck, D. W. and Leahy, R. M. (2002). BrainSuite: An automated cortical surface identification tool. *Medical Image Analysis*, 6, 129–142.

Shaw, P. *et al.* (2007). Cortical morphology in children and adolescents with different apolipoprotein E gene polymorphisms: an observational study. *The Lancet Neurology*, 6, 494–500.

Shi, J. *et al.* (2014). Genetic influence of apolipoprotein E4 genotype on hippocampal morphometry: an $N = 725$ surface-based Alzheimer's disease neuroimaging initiative study. *Human Brain Mapping*, 35, 3903–3918.

Shiino, A. *et al.* (2006). Four subgroups of Alzheimer's disease based on patterns of atrophy using VBM and a unique pattern for early onset disease. *NeuroImage*, 33, 17–26.

Sperling, R. A. *et al.* (2009). Amyloid deposition is associated with impaired default network function in older persons without dementia. *Neuron*, 63, 178–188.

Smith, S. M. *et al.* (2009). Correspondence of the brain's functional architecture during activation and rest. *Proceedings of the National Academy of Sciences of the United States of America*, 106, 13040–13045.

Szczepanski, S. M. and Knight, R. T. (2014). Insights into human behavior from lesions to the prefrontal cortex. *Neuron*, 83, 1002–1018.

Taylor, J. L. *et al.* (2014). APOE-epsilon4 and aging of medial temporal lobe gray matter in healthy adults over 50. *Neurobiology of Aging*, 35, 2479–2485.

Uddin, L. Q. (2015). Salience processing and insular cortical function and dysfunction. *Nature Reviews Neuroscience*, 16, 55–61.

Walhovd, K. B. *et al.* (2011). Consistent neuroanatomical age-related volume differences across multiple samples. *Neurobiology of Aging*, 32, 916–932.

Watanabe, T. *et al.* (2013). A pairwise maximum entropy model accurately describes resting-state human brain networks. *Nature Communications*, 4, 1370.

Westlye, L. T., Grydeland, H., Walhovd, K. B. and Fjell, A. M. (2011). Associations between regional cortical thickness and attentional networks as measured by the attention network test. *Cerebral Cortex*, 21, 345–356.

Wikenheiser, A. M. and Redish, A. D. (2012). Hippocampal sequences link past, present, and future. *Trends in Cognitive Sciences*, 16, 361–362.

Wishart, H. A. *et al.* (2006). Regional brain atrophy in cognitively intact adults with a single APOE ε4 allele. *Neurology*, 67, 1221–1224.

Yao, Z. *et al.* (2015). A FDG-PET study of metabolic networks in apolipoprotein E ε4 allele carriers. *PloS One*, 10, e0132300.

Zhuang, L. *et al.* (2012). Microstructural white matter changes in cognitively normal individuals at risk of amnestic MCI. *Neurology*, 79, 748–754.

https://doi.org/10.1017/S1041610216000624 Published online by Cambridge University Press